https://doi.org/10.5194/egusphere-2023-2835
Preprint. Discussion started: 8 January 2024

Characteristics and sources of VOCs and the O_3-NO_x-VOCs relationships in the central plain city, China

Dong Zhang[1,3], Xiao Li[2,3], Minghao Yuan[4], Yifei Xu[4], Qixiang Xu[2,3], Fangcheng Su[2,3], Shenbo Wang[2,3], Ruiqin Zhang[2,3,*]

1 College of Chemistry, Zhengzhou University, Zhengzhou 450001, China

2 School of Ecology and Environment, Zhengzhou University, Zhengzhou, 450001, China

3 Institute of Environmental Sciences, Zhengzhou University, Zhengzhou 450001, China

4 Environmental Protection Monitoring Center Station of Zhengzhou, Zhengzhou 450007, China

Correspondence: Ruiqin Zhang (rqzhang@zzu.edu.cn)

Abstract:

Volatile organic compounds (VOCs) are important precursors of ozone (O_3) generation. Understanding the characteristics, and emission sources of VOCs, and the relationship between VOCs and O_3 during O_3 pollution are of great significance for O_3 pollution control. This study investigated the characteristics, sources, and effects of VOCs on O_3 formation in Zhengzhou, Henan Province from 1st to 30th June 2023, and provided recommendations for O_3 emission reduction strategies. Two O_3 pollution events occurred during the observation period. During the observation period, the concentration of Total VOCs (TVOCs) varied from 9.9 to 60.3 ppbv, with an average of 22.8 ± 8.3 ppbv. The average concentration of TVOCs in the two pollution events were higher than that on the clean days. Six major VOCs sources were identified by using the Positive Matrix Factorization model. Vehicular exhaust (28%), solvent usage (27%), and industrial production (22%) were the main sources. An observation-based mode was applied to explore the O_3-precursors relationship and observation-oriented O_3 control strategies. The results of relative incremental reactivity (RIR) and empirical kinetics modeling approach showed that the O_3 formation in Zhengzhou in June was in anthropogenic VOCs (AVOCs)-limited regimes. VOCs with the largest RIR values, while NO_x had a negative RIR value. It was worth noting that the sensitivity of O_3 generation to biogenic VOCs (BVOCs) was greater than that of AVOCs. From the perspective of the reduction effect, the reduction ratios of AVOCs/NO_x should be no less than 3:1, which was conducive to the reduction of O_3 formation.

Keywords: Emission reduction strategies; Positive Matrix Factorization; Relative incremental reactivity; The observation-based model; Empirical kinetics modeling approach

https://doi.org/10.5194/egusphere-2023-2835
Preprint. Discussion started: 8 January 2024

1 Introduction

In recent years, ozone (O_3) pollution has become increasingly prominent in China, especially in urban areas (Liu et al., 2023a; Zhao et al., 2021; Yan et al., 2023; Sicard et al., 2020). O_3 pollution has become an important factor affecting the ambient air quality (Zhang et al., 2023). Volatile organic compounds (VOCs), as an important precursor of O_3 and secondary organic aerosols, widely exist in the atmospheric environment and participate in many photochemical reactions, which have an important impact on atmospheric oxidation capacity and air quality (Zhu et al., 2021). Some VOCs are also air toxics (Billionnet et al., 2011), such as benzene, trichloroethylene, and chloroform (Lerner et al., 2012). Long-term exposure to higher concentrations of VOCs can lead to acute or chronic risks (He et al., 2015). Therefore, it is necessary to continue to carry out VOCs monitoring activities in O_3 pollution areas to analyze O_3 concentration levels, sources, and effects on O_3 generation.

The concentration of VOCs is affected by background concentration, weather conditions (Mo et al., 2015), emission sources, terrain conditions (Liu et al., 2016), and extent of pollutant transport (Shao et al., 2009). In addition, under meteorological conditions with higher temperature, VOCs exhibit photochemical losses during dispersion and regional transport (Zou et al., 2023; Liu et al., 2023a; Liu et al., 2020). As a result, the ambient VOC concentration of course varies with the locality and season. For example, in typical coastal areas of Ningbo, the seasonal variation of VOCs concentration was winter > spring > Autumn > summer (Huang et al., 2023). The coastal areas of Shandong Province had the highest value in winter (28.5 ± 15.1 ppbv) and the lowest value in autumn (14.5 ± 7.6 ppbv) (Huang et al., 2023). The average summer TVOCs concentration in the suburbs of Jinan (12.0 ± 5.1 ppbv) (Liu et al., 2023c) was lower than that in the suburbs of Beijing (18.3±8.9 ppb), and much lower than that in the central city of Beijing (44.0 ± 28.9 ppbv) (Wu et al., 2023). The average TVOCs concentration (21.7 ppbv) in the O_3 pollution period in Tianjin is 12% higher than that in the non-O_3 pollution period (Liu et al., 2023a).

VOCs are emitted from various sources including anthropogenic sources and biogenic sources (Chameides et al., 1992) as well as secondary generation through photochemical reactions (Yuan et al., 2012). The main sources of VOCs include motor vehicle emissions, industrial processes, solvent usage, fuel evaporation, combustion, and biogenic emissions (Wu et al., 2016; Prendez et al., 2013; Watson et al., 2001). Biogenic emission is mainly affected by temperature and radiation conditions (Li et al., 2020). Biogenic emissions are therefore higher during hotter months, especially in summer (Pacifico et al., 2009; Xu et al., 2023). Urban areas are greatly affected by anthropogenic sources (Zhang et al., 2023; Goldstein and Galbally, 2007). In different regions, the main contribution sources of VOCs are different. For example, the main anthropogenic

https://doi.org/10.5194/egusphere-2023-2835
Preprint. Discussion started: 8 January 2024

VOCs (AVOCs) sources in the Yangtze River Delta region of China are vehicle and solvent evaporation (Xu et al., 2023). The Pearl River Delta region is mainly affected by solvent use, liquefied petroleum gas use, and vehicle exhaust. Atmospheric VOCs in Beijing are greatly affected by motor vehicle emission sources and combustion sources (Liu et al., 2021; Zhang et al., 2020). Huang et al. (2023) reported that plastic synthesis, industrial processes, organic solvents, dyeing, traffic emissions, and pesticides were identified as the main sources of VOCs in Ningbo City in the coastal area (Liu et al., 2023b). Since different emission sources have different contributions to VOCs and thus have different impacts on the generation of O_3 (Zhang et al., 2023), it is necessary to investigate the sources of VOCs in different cities.

Designing a reasonable and effective precursor emission control strategy is crucial to control the photochemical generation of O_3 (Yang et al., 2021). The relationship between O_3 and precursors is nonlinear (Chameides et al., 1992), and precursor emission reduction strategies need to be dynamically adjusted based on the actual sensitivity of O_3 formation (Chu et al., 2023; Lin et al., 2005). The observation-based model (OBM) is a widely used tool to analyze O_3-NO_x-VOCs sensitivity (Zhang et al., 2008; Nelson et al., 2021; Cardelino and Chameides, 1995). Several studies in China have analyzed the sensitivity of O_3 to precursors and control scenarios. For example, O_3 in the central area of the Yangtze River Delta is in a VOCs-limited regimes, and AVOCs play a leading role in the formation of O_3 (Liu et al., 2023b). Chengdu is in a typical VOCs restricted area, so VOCs emission reduction helps to prevent and control O_3 pollution, and the emission reduction scenario based on VOCs source showed that the emission reduction ratio of VOCs to NO_2 needs to reach more than 3 to achieve prevention of O_3 pollution (Chen et al., 2022b). Xie et al. (2021) found that controlling AVOCs in Leshan, a non-provincial capital city in southwest China, can effectively reduce the photochemical generation of O_3, and pointed out that the best emission reduction strategy for VOCs and NO_x should be 3:1. In addition, the generation of O_3 in areas such as Shanghai (Lu et al., 2023), Rizhao (Zhang et al., 2023), and Nanjing (Mozaffar et al., 2021) is generally limited by VOCs. However, in the United States and European countries, O_3 formation gradually transitioned from VOCs-limited regime to NO_x-limited regime (Nopmongcol et al., 2012; Ring et al., 2018; Goldberg et al., 2016).

Zhengzhou is the capital city of Henan Province and an important transportation hub in China. High population density levels, large vehicle ownership (MPS, 2022) and complex industrial structures determine the complexity of VOCs emission sources. In recent years, Zhengzhou's O_3 pollution has increasingly intensified, becoming one of the cities with the highest O_3 pollution in central China (Wang et al., 2023b;Min et al., 2022). From 2020 to 2022, the annual 90th percentile of the mean daily maximum 8 h average O_3 (O_3-8H-90per) published by Zhengzhou Ecological Environment Bureau were 182, 177 and 178 μg/m^3,

https://doi.org/10.5194/egusphere-2023-2835
Preprint. Discussion started: 8 January 2024

respectively, which were 10% to 13% higher than the National Ambient Air Quality Grade II Standard (160 μg/m^3) (https://sthjj.zhengzhou.gov.cn/, last access: June, 2023). Some studies have analyzed the concentration levels, sources, and impact of VOCs on O_3 in Zhengzhou (Zeng et al., 2023; Wang et al., 2023b; Min et al., 2022). Wang et al. (2022) analyzed the sensitivity of O_3 to precursors and found that in July with low O_3 levels in Zhengzhou, O_3 formation was in a VOCs-limited state, while on O_3 pollution accumulation and persistence days, O_3 formation was in a transitional state. Yu et al. (2021) showed that Zhengzhou was under a VOCs-sensitive regime in September. The above studies all show that it is important to study the emission reduction of precursors to control O_3 generation. However, there is still a lack of relevant research on June, the month with the heaviest O_3 pollution in Zhengzhou. In order to effectively solve the increasingly serious trend of O_3 pollution in Zhengzhou, it is necessary to give priority to and strengthen the research of Zhengzhou area, especially during the period of high O_3 pollution. Therefore, it is necessary to continue to pay attention to the pollution levels of O_3 and precursors in Zhengzhou and further explore the relationship between them.

In this study, we conducted an online measurement of VOCs in June, when O_3 pollution was severe in Zhengzhou. The concentration, composition, and diurnal variation of VOCs in the atmosphere were analyzed. The main sources of VOCs were discussed by using ratio method and Positive Matrix Factorization (PMF) model. OBM was used to analyze the sensitivity of O_3-VOCs-NO_x and consequently the emission reduction strategy of precursors to control O_3 concentration was proposed. This study establishes a collaborative control strategy for atmospheric VOCs, which is of great significance for the control of atmospheric O_3 pollution in Zhengzhou.

2. Materials and methods

2.1 Sampling site

The monitoring site is on the roof (about 20 m above ground) of the building at Zhengzhou Environmental Protection Monitoring Centre Station (34.75° N, 113.60° E) (Fig. S1). The sampling site is surrounded by residential areas, commercial areas, and office buildings, and there are no obvious atmospheric pollution sources nearby, which is a typical urban site. The sampling site is surrounded by roads and vegetation, and the sampling may be affected by motor vehicle emissions and plant emissions.

2.2 Sample collection and chemical analysis

115 VOCs species concentrations were observed with a gas chromatography-mass spectrometer, GC-MS (TH-PKU 300B, Wuhan Tianhong Instrument, China), which adopted detection technology of ultralow-temperature preconcentration combined with GC-MS/ flame ionization detector. Details of the device can be

https://doi.org/10.5194/egusphere-2023-2835
Preprint. Discussion started: 8 January 2024

found in our previous study (Zhang et al., 2021). Also the study conducted the simultaneous online measurements of hourly concentrations of particulate matter ($PM_{2.5}$ and PM_{10}), other trace gases (CO, O_3, NO, and SO_2), and meteorological data (temperature (T), relative humidity (RH), atmospheric pressure, and wind speed (WS) and wind direction (WD).

2.3 PMF model

The PMF 5.0 is an advanced multivariate factor analysis tool (USEPA, 2014), which can be used to identify the sources of VOCs (Norris et al., 2014). PMF model is expressed as follows:

$$X_{ij}=\sum_{k=1}^{p} g_{ik}f_{kj}+e_{ij} \quad (1)$$

where, *i, j,* and *k* represent the i^{th} sample, the j^{th} chemical species, and the k^{th} factor, respectively; *X* represents the chemical species concentration measured in the sample; *g* is the species contribution; *f* is the species fraction; and *e* is the residual matrix.

The number of factors is obtained by minimizing objective residual function Q: as follows:

$$Q=\sum_{i=1}^{n}\sum_{j=1}^{m}\left[\frac{X_{ij}-\sum_{k=1}^{p} g_{ik}f_{kj}}{u_{ij}}\right]^2 \quad (2)$$

Where μ^{ij} is the sample data uncertainty.

The sample data uncertainty is calculated by Equations (3) and (4). If the data concentration is less than method detection limit (MDL), Equation (3) is used. Otherwise, Equation (4) is used.

$$Unc=\frac{5}{6}\times MDL \quad (3)$$

$$Unc=\sqrt{(Error\ Fraction\ \times concentration)^2+(0.5\times MDL)^2} \quad (4)$$

where Error Fraction represent the precision (%) of each species;

Species with high proportions of missing samples or concentration values more than 25% below MDLs were excluded, while VOCs serving as typical tracers of emission sources were included (USEPA, 2014), and VOCs with short atmospheric lifetimes were excluded (Callén et al., 2014; Guo et al., 2011). In this study, 29 out of 115 VOCs collected over the sampling period was analyzed by the PMF model. In this study, a seven-factor solution ($Q_{true}/Q_{theoretical}$ = 3.42; and Fpeak = 0) was chosen (Fig. S2).

2.4 Conditional bivariate probability function analysis

The conditional probability function (CPF) is a new source identification tool, which can be used to identify local emission sources of pollutants (Xie and Berkowitz, 2006). CPF analysis methods were used to

https://doi.org/10.5194/egusphere-2023-2835
Preprint. Discussion started: 8 January 2024

locate the possible direction of different pollutants in this study. The CPF is defined as (Song et al., 2007):

$$CPF = \frac{m_{\Delta\Theta}}{n_{\Delta\Theta}} \quad (7)$$

Where $\Delta\theta$ is the wind sector $\Delta\theta$; $m_{\Delta\theta,}$ the number of samples; and $n_{\Delta\theta}$ is the total number of samples in the WD-WS.

2.5 OBM

OBM based on the Master Chemical Mechanism (MCM v3.3.1; http://mcm.leeds.ac.uk/MCM/) was employed to estimate the effect of changes of what in O_3 precursors (Liu et al., 2022). Detailed information about OBM can be viewed in previous studies (Chu et al., 2023; Ling et al., 2011). Briefly, OBM assumes a good mix of emitted pollutants and is independent of emission inventories and meteorological data, combined with atmospheric chemical mechanisms, simulates the O_3 production rate and the corresponding O_3 concentration at a given time (Kleinman, 2000; Qiao et al., 2023). The relative incremental reactivity (RIR) was computed through OBM to evaluate the sensitivity of the photochemical production of O_3 to changes in the concentration of individual precursors within a given region (Ling et al., 2013; Cardelino and Chameides, 2000), which can be calculated from Eq. (8):

$$RIR(X) = \frac{[P_{O_3}(X) - P_{O_3}(X - \Delta X)]/P_{O_3}(X)}{\Delta S(X)/S(X)} \quad (8)$$

where X is the specific precursor of O_3; $P_{O_3}(X)$ and $P_{O_3}(X - \Delta X)$ are the net production of O_3 simulated by the OBM; and $\Delta S(X)/S(X)$ is the change in the concentration of $S(X)$. The large change in primary pollutants (>20%) deviates greatly from the base scenario and is not representative of the current situation. Therefore, the concentration changes of $\Delta S(X)/S(X)$ were assumed to be 20%. In this study, the S for AVOCs and NO_x were reduced by 0-100%. The relative change of $P_{O_3}(X)$ with S(AVOCs) and S(NO_x) can be expressed by the isogram of $P_{O_3}(X)$.

The concentrations of, trace gases (SO_2, O_3, CO, and NO), and meteorological parameters (T, RH, and WS) with 1 h time resolution were used as constraints in this model. At the same time, the concentrations of 75 VOCs observed with 1 h time were selected for input into the model because these 75 VOCs were included in MCM v3.3.1. The photolysis frequency ($J(H_2O_2)$, $J(O_1D)$) and planetary boundary layer are the default values. Then, the differential equation is calculated with a time resolution of 1 h, and the mixing proportion of various photochemical reaction products, intermediates and free radicals can be obtained.

To evaluate the performance of this model, the consistency index (IOA) was used in this study (Huang et al., 2005):

$$IOA = 1 - \frac{\sum_{i=1}^{n}(O_i - M_i)^2}{\sum_{i=1}^{n}(|O_i - \overline{O}| + |M_i - \overline{O}|)^2} \quad (9)$$

https://doi.org/10.5194/egusphere-2023-2835
Preprint. Discussion started: 8 January 2024

where O_i, M_i, and $\overline{O}$ represent the hourly values of observation, the simulation, and the average of observations, respectively. The IOA values for O_3 was 0.6 in this study, indicating the acceptable performance of this model.

3 Results and discussions

3.1 General characteristics

3.1.1 VOCs concentrations and composition

According to the Chinese National Ambient Air Quality Standards (NAAQS), the grade II threshold of the maximum daily 8-h average (MDA8) of O_3 was 160 μg/m^3 (~75 ppbv). Two O_3 pollution events were found over 160 μg/m^3, which were named case 1 (8th-17th Jun.) and case 2 (20th-27th Jun.). Meanwhile, there were also O_3 pollution events on 6th Jun. and 29th-30th Jun., but were not discussed in this study due to the short pollution process. The rest of the observation periods were clean days. Figure. 1 shows the time series of the concentration of TVOCs, O_3 8-h moving average, SO_2, $PM_{2.5}$, NO_x, CO, and meteorological parameters (WD, WS, T, and RH) from 1st to 30th June 2023. The gray areas in Fig. 1 are O_3 pollution events, and the remaining areas are non-polluting processes (clean days). During the observation, O_3 polluted days were 22 days, accounting for 73%.

During the observation period, the average wind speed (1.3 ± 0.9 m/s) was relatively low, which was not conducive to the dispersion. The mean RH (52 ± 19%) was low, and the mean temperature (28.9 ± 4.6 °C) was high. The meteorological conditions of high temperature and low humidity were conducive to the occurrence of photochemical pollution. The maximum daily 8-h moving average (MDA8) of O_3 reaching 229 μg/m^3. The mean concentrations of SO_2, NO_2, CO, PM_{10} and $PM_{2.5}$ were 4.4 ± 3.3 μg/m^3, 26.5 ± 17.9 μg/m^3, 0.6 ± 0.2 mg/m^3, 59.6 ± 26.5 μg/m^3 and 22.9 ± 7.1 μg/m^3, respectively. All of them were lower than the ambient air quality standard value. The average concentration of TVOCs was 22.8 ± 8.3 ppbv.

During the Case 1 process, O_3 pollution continued for 10 days. The average RH and temperature were 41 ± 16% and 29.9 ± 4.1 °C, respectively, and the average WS was 1.3 ± 0.8 m/s. The concentration of MDA8 O_3 reached a maximum of 228 μg/m^3 (June 11) during the pollution period, which was higher than the grade II threshold of MDA8 O_3. In Case 1, the mean concentrations of SO_2, NO_2, CO, PM_{10} and $PM_{2.5}$ were 6.1 ± 4.1 μg/m^3, 27.4 ± 19.5 μg/m^3, 0.6 ± 0.1 mg/m^3, 69.1 ± 31.5 μg/m^3 and 25.6 ± 6.8 μg/m^3, respectively. The average concentration of TVOCs during this process was 24.1 ± 8.9 ppbv. In Case 2, O_3 pollution occurred continuously for 8 days. The average RH and average temperature were 50 ± 14% and 31.2 ± 2.9 °C. The average concentrations of TVOCs (22.5 ± 7.4 ppbv), SO_2 (2.7 ± 2.1 mg/m^3), NO_2 (24.9 ± 12.3 mg/m^3), CO

https://doi.org/10.5194/egusphere-2023-2835
Preprint. Discussion started: 8 January 2024

209 (0.6 ± 0.1 mg/m^3), PM_{10} (61 ± 19 mg/m^3), and $PM_{2.5}$ (24 ± 7 mg/m^3) in Case 2 were all lower than those in
210 Case 1 process.

211 The average RH (65 ± 17%) on clean days was higher than those during Case1 and Case2 events, while
212 the average temperature (26.0 ± 4.8 °C) was lower than those during Case1 and Case2 events. High
213 temperature and low humidity are more conducive to O_3 pollution (Chen et al., 2020; Zhang et al., 2015). In
214 addition to SO_2 and CO, the average concentration of TVOCs, NO_2, PM_{10}, and $PM_{2.5}$ was lower than that of
215 the O_3 pollution processes.

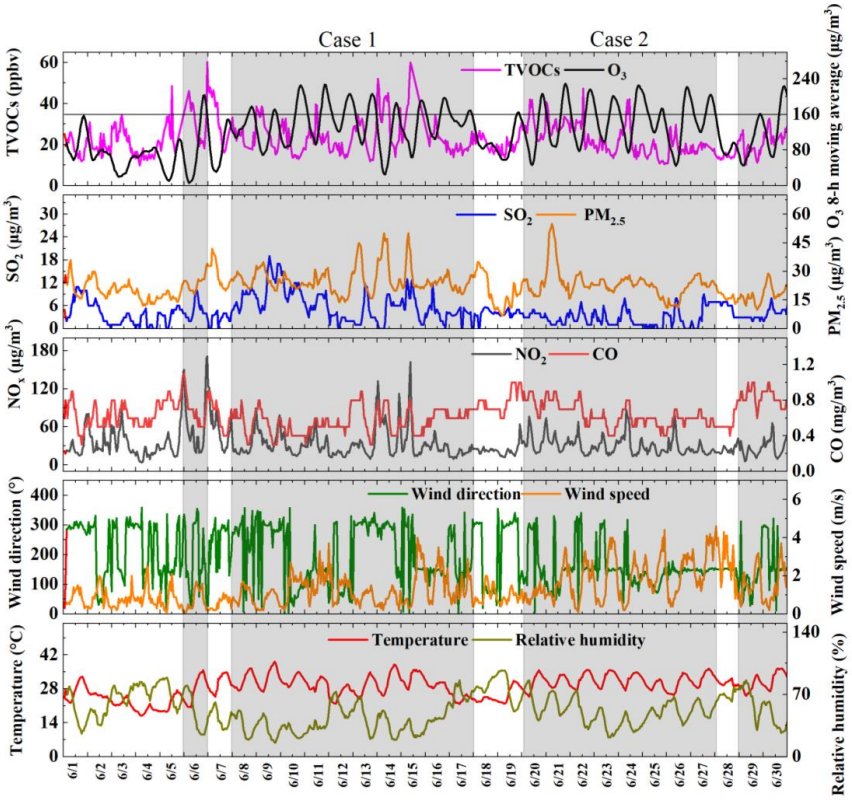

216

217 **Fig. 1.** Hourly concentrations of TVOCs, O_3 8-h moving average, SO_2, $PM_{2.5}$, NO_x, CO, and meteorological
218 parameters (WD, WS, T, and RH) during the sampling period (gray regions represent O_3 pollution processes).

219 The means and standard deviations of VOCs groups during different processes were listed in Table 1.
220 During the entire period, the concentration of TVOCs varied from 10 to 60 ppbv, with an average mean of
221 23.0 ± 8.0ppbv. A similar level of VOCs concentration was observed between Case 1 (24.0 ± 9.0 ppbv) and
222 Case 2 (23.0 ± 7.0 ppbv). The TVOCs concentrations on clean days were relatively low (21 ± 7. ppbv).
223 Furthermore, nearly all VOCs groups in O_3 pollution events were higher than those on clean days.

224 As for the entire sampling period, alkanes (10.0 ± 4.4 ppbv), OVOCs (4.5 ± 1.3 ppbv), and halocarbons
225 (4.3 ± 1.9 ppbv) were the most abundant VOC groups, accounting for 44, 20 and 19% of the TVOCs,

https://doi.org/10.5194/egusphere-2023-2835
Preprint. Discussion started: 8 January 2024

226 respectively, followed by alkenes (9%), aromatics (5%), alkenes (5%), OVOCs (7%), alkyne (7%) and sulfide
227 (1%). During the two O_3 pollution events, alkanes being the highest VOCs group contributed 41% (Case 1),
228 and 43% (Case 2) to the TVOCs, respectively. Alkanes were the most abundant VOCs during the observation
229 period, in part due to the presence of alkanes emission sources around the observation site (e.g., civilian
230 combustion and motor vehicle emissions) and the low photochemical reactivity of alkanes (Mozaffar et al.,
231 2020). Even if on clean days, alkanes (9.6 ± 3.9 ppbv) were also the highest group (46%), and halocarbons
232 (19%) and OVOCs (19%) were another two major groups.
233
234 **Table 1.** Concentrations of VOCs during different processes in Zhengzhou, ppbv.

Species	Entire period (n = 652)		Case 1 Jun. 8 - 17 (n = 201)		Case 2 Jun. 20 - 27 (n = 184)		Clean days (n = 224)	
	Range	Average ± SD	Range	Average ± SD	Range	Average ± SD	Range	Average ± SD
Alkanes	3.6 - 30.7	10.0 ± 4.4	4.2 - 28.3	10.0 ± 4.6	3.6 - 24.6	9.6 ± 4.1	4.6 - 22.2	9.6 ± 3.9
Alkenes	0.4 - 10.7	2.0 ± 1.2	0.6 - 10.7	1.9 ± 1.2	0.6 - 10.7	2.5 ± 1.4	0.4 - 4.0	1.7 ± 0.7
Aromatics	0.3 - 5.0	1.1 ± 0.7	0.4 - 4	1.2 ± 0.8	0.3 - 3.1	1.1 ± 0.6	0.3 - 4.4	1.1 ± 0.6
Halocarbons	1.8 - 31.1	4.3 ± 1.9	2.0 - 10.6	4.5 ± 1.8	2.2 - 8.8	4.2 ± 1.4	1.8 - 31.1	3.9 ± 2.2
OVOCs	1.8 - 9.7	4.5 ± 1.3	3.4 - 9.7	5.3 ± 1.2	2.0 - 8.1	4.4 ± 1.1	1.8 - 8.6	3.9 ± 1.2
Sulfide	0.0 - 1.5	0.1 ± 0.2	0.0 - 1.5	0.2 ± 0.3	0.0 - 0.5	0.1 ± 0.1	0.0 - 1.0	0.1 ± 0.1
Alkyne	0.1 - 3.7	1.1 ± 0.6	0.2 - 3.2	1.1 ± 0.6	0.2 - 3.2	1.0 ± 0.5	0.1 - 3.7	1.0 ± 0.7
TVOCs	9.9 - 60.3	22.8 ± 8.3	0 - 60.0	24.1 ± 8.9	10.5 - 47.3	22.5 ± 7.4	9.9 - 48.5	20.8 ± 7.2

235 n: Total sampling numbers for each period

236 Figure 2 illustrates the top fifteen VOCs species during two O_3 pollution events and clean days. Ethane,
237 propane, n-butane, isopentane, isobutane, n-hexane, and n-pentane were the most abundant of the alkanes
238 during each of the entire observation period. Ethane is a major component of natural gas (NG) (Thijsse et al.,
239 1999), propane, n-butane, and isobutane are important tracers of liquefied petroleum gas (LPG) (Tsai et al.,
240 2006; An et al., 2014). N-hexane is mainly from solvent emissions. Ethylene, propylene, and isoprene were
241 the most abundant of the alkenes. Ethylene and propylene mainly come from biomass burning (Andreae and
242 Merlet, 2001). Isoprene mainly comes from plants (Brown et al., 2007). Acetylene also had a high level, which
243 is the tracer of incomplete combustion (Blake and Rowland, 1995). Benzene and toluene were the most
244 abundant of the aromatics, which are mainly from solvent emissions, vehicular exhaust, and industry processes
245 (Seila et al., 2001; Mo et al., 2015). Dichloromethane was the most abundant species of the halohydrocarbons,
246 which is an important species in solvent usage (Huang et al., 2014). The acetone was the most abundant species
247 in OVOCs, which has complex atmospheric sources and is mainly attributed to vehicular emission and
248 secondary formation (Guo et al., 2013; Watson et al., 2001). The concentration of acetone in the two pollution
249 processes was significantly higher than that in the clean day as also reported by others (Guo et al., 2013),

https://doi.org/10.5194/egusphere-2023-2835
Preprint. Discussion started: 8 January 2024

indicating that the pollution process had a strong photochemical reaction e.g., photo-oxidation of i-butene to acetone (Guo et al., 2013). Therefore, vehicle exhaust, solvent use, combustion, biogenic emission, and industrial processes are important sources of VOCs at observation sites, as also illustrated in the following PMF source apportionment.

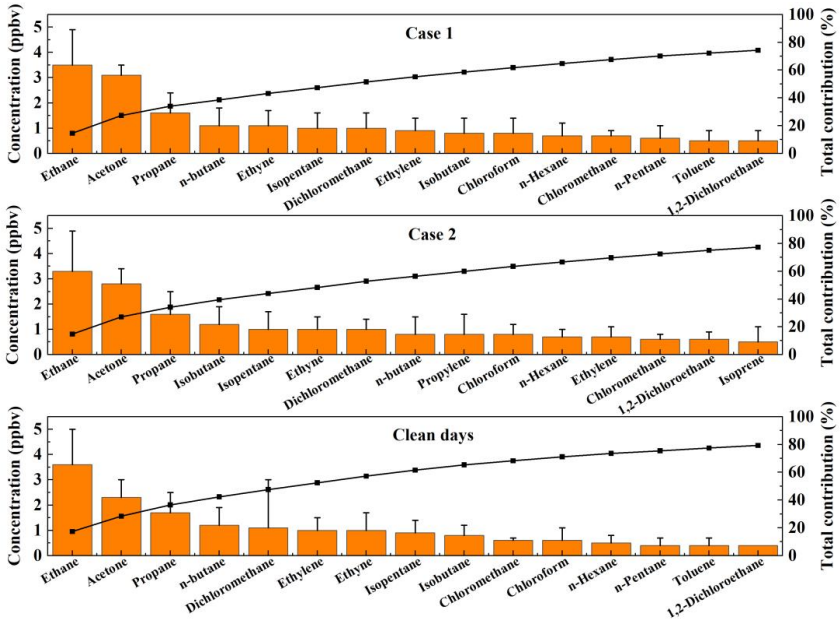

Fig. 2. Comparisons of the top fifteen VOCs during different processes, ppbv. Error bars are standard deviations.

3.1.2 Diurnal variations of VOCs, O_3, and NO_x

The concentration characteristics of pollutants in the atmosphere are affected by the atmospheric boundary layer variation pattern, photochemical reaction intensity, and emission of pollution sources (Wang et al., 2023a). Major VOCs, O_3, and NO_x were selected, and their daily changes were analyzed, as shown in Fig. S3. The diurnal variation of O_3 concentration shows unimodal characteristics. During the day, with the increase in temperature and light intensity, the concentration of O_3 gradually increased and reached a peak at about 14:00, and then the concentration gradually decreased. Higher O_3 production during the day indicates a strong photochemical reaction. The diurnal variation of ethane, propane, isobutane, n-butane, isopentane, n-pentane, ethylene, propylene, acetylene, benzene, and toluene were similar, showing low concentrations in the daytime and high concentrations in the evening. This is associated with a higher boundary layer and strong photochemical reactions during the day (Tang et al., 2007). The elevated boundary layer is conducive to the dispersion of VOCs and other pollutants (Bon et al., 2011; Chen et al., 2022a), while the strong photochemical reaction will consume VOCs (Xia et al., 2014; Zhang et al., 2018). In addition, the peak concentration of these

https://doi.org/10.5194/egusphere-2023-2835
Preprint. Discussion started: 8 January 2024

VOCs appeared in the morning and evening (7:00-8:00 and 23:00-24:00), and the daily change was consistent with NO_x, indicating that the emission of these VOCs was greatly affected by motor vehicle emissions and fuel combustion. Higher VOCs and NO_x concentrations at night may be caused by heavy traffic emissions for traditional nighttime activities in the city. Isoprene is a typical tracer of plant emissions, which are highly dependent on temperature and solar radiation (Pacifico et al., 2009). Therefore, the concentration of isoprene increases significantly during the day (7:00-20:00) and decreases significantly at night. It is worth noting that the concentration of isoprene showed a bimodal characteristic. Two peaks occur at 10:00 AM and 15:00 PM (local standard time). Previous studies have shown that the rate at which plants emit isoprene decreases when temperatures exceed 40 °C (Guenther et al., 1993). Therefore, the drop in isoprene concentrations seen at noon may be due to excessive temperatures affecting biogenic emissions. Acetone is a common VOC and comes from a wide range of sources, mainly from vehicle emissions, industrial production, and secondary formation (Sha et al., 2021). Acetone remained in high concentration throughout the day, and there was no obvious diurnal variation, suggesting that there might be primary acetone sources near the site, which concealed the acetone peak at the daytime produced by photochemical reaction (Guo et al., 2013). Dichloromethane mainly comes from solvent use, and its high concentration was mainly concentrated at night (23:00-5:00), which might be related to the longer atmospheric lifetime of dichloromethane and the lower boundary layer height at night (Li et al., 2018; Chen et al., 2022a).

3.2 Sources of VOCs

3.2.1 Diagnostic ratios

Ratios of specific VOCs can be used to assess the initial emission source of VOCs or the degree of photochemical reaction (Miller et al., 2012; An et al., 2014). The ratios of isobutane/n-butane, toluene/benzene (T/B), and m-p-xylene/ethylbenzene (X/E) are discussed in this study (Fig. 3).

In Case 1, Case 2, and clean days, the Pearson coefficients of isopentane and n-pentane were 0.7, 0.94, and 0.6, respectively, indicating a strong correlation that the two substances had a common emission source. Isopentane/n-pentane ratios of 0.8-0.9, 2.2-3.8, 1.5-3.0 and 1.8-4.6 (Fig. 3a), indicate that isopentane and n-pentane come from natural NG, vehicle emissions, liquid gasoline, and fuel evaporation, respectively (Zhang et al., 2016; An et al., 2014). In this study, the ratios of case 1, case 2, and clean days were 0.7, 2.5, and 1.1, respectively. It suggests that isopentane and n-pentane may come from NG emissions, vehicular exhaust, and liquid gasoline, respectively.

The T/B ratio can be used to distinguish between coal and biomass combustion (0.2-0.6), motor vehicle emissions (~2.0) (Liu et al., 2008), industrial processes (3.0-6.9) (Zhang et al., 2016) and fuel evaporation

https://doi.org/10.5194/egusphere-2023-2835
Preprint. Discussion started: 8 January 2024

(~4.1) (Dai et al., 2013). In this study, the T/B ratio of the two O_3 pollution events was 1.7 and 1.4 (Fig. 3b), respectively, indicating that combustion and vehicle emissions were the main sources of benzene and toluene emissions (Hong et al., 2019).

Since m/p-xylene and ethylbenzene share a common source, but differ from the OH radical reaction rate constant, X/E can be used to determine the photochemical age of air masses and the transport path (Miller et al., 2012; Yurdakul et al., 2018). During the pollution events and clean days, m, p-xylene, and ethylbenzene showed a strong positive correlation (r = 0.9) (Fig. 3c), indicating that m/p-xylene and ethylbenzene came from a common emission source. Previous studies have shown that VOCs are transported from inner urban areas when the E/X ratio is 0.3-0.4, and VOCs are transported from distant sources when the ratio is significantly higher than 0.3 (Monod et al., 2001). In this study, the E/X ratios of the two pollution events and clean days were 0.5, indicating that the air mass measured at the observation point was affected by air mass transport.

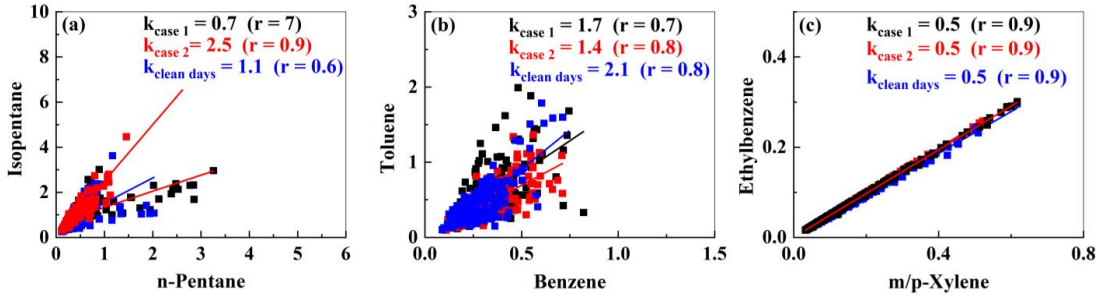

Fig. 3. Correlations (k = slope) between compounds with different observation periods.

3.2.2 Source apportionment

In this study, EPA PMF5.0 was used to analyze the source profile and species percentage of each source during the observation period to determine the relative contribution of each potential source, as shown in Fig. 4. Seven factors were determined by the model, namely combustion, industrial production, biogenic emission, vehicular exhaust, LPG/NG, solvent use 1, and solvent use 2. Detailed analysis is followed.

Factor 1 was characterized by high percentages of acetylene (76%), ethane, propane, ethylene benzene, and toluene. Acetylene is a typical tracer of coal burning (Barletta et al., 2005). Ethane, propane, and ethylene are typically tracers of incomplete combustion (Guo et al., 2011; Ling et al., 2011). Therefore, Factor 1 was classified as combustion. The CPF plots indicate that the contributing direction was northwest at about 2 m/s (Fig. S4a).

Factor 2 was rich in C4-C6 alkanes, aromatics, (toluene, ethylbenzene, m/p-Xylene, o-xylene, and 1,2,4-trimethylbenzene, and halocarbons (1, 2-dichloroethane and 1, 2-dichloropropane). Previous studies have

https://doi.org/10.5194/egusphere-2023-2835
Preprint. Discussion started: 8 January 2024

shown that these species were all related to industrial production. Therefore, Factor 2 was classified as industrial production. The CPF plots indicated that a local source under a low wind speed of < 1 m/s was the dominant source (Fig. S4b).

Factor 3 was characterized by high percentages (83%) of isoprene, a typical tracer of biogenic emission (Brown et al., 2007). The high temperature and strong radiation in summer are more conducive to the biogenic emission of isoprene (Liu et al., 2016). Therefore, Factor 3 was classified as a biogenic emission. The CPF plots indicated that the southwest was the dominant source direction under wind speeds below 2 m/s (Fig. S4c).

Factor 4 was characterized by high percentages of C2-C6 alkanes (such as ethane, propane, isobutane, n-butane, isopentane, n-pentane, 2, 2-dimethylbutane, and 2, 3-dimethylbutane), benzene, toluene, ethylbenzene, and m/p-xylene), which are related to vehicular emission (Jorquera and Rappenglück, 2004; Song et al., 2007; Chen et al., 2014). Therefore, Factor 4 was classified as vehicular exhaust. The CPF plots indicated that a local source under a low wind speed was the dominant source, which might be related to the large amount of traffic on the main roads in the southern and western directions direction (Fig. S4d).

Factor 5 was characterized by high percentages of ethane, propane, isobutane, and propylene, which are the main components of LPG/NG (Shao et al., 2016; Song et al., 2007; Na et al., 2001). Therefore, Factor 5 was classified as LPG/NG source. The CPF plots showed the dominant source directions of this factor were east at 1-2 m/s (Fig. S4e).

Factor 6 was characterized by high percentages of chloromethane, dichloromethane, tetrachloromethane, 1,2-dichloroethane, 1,2-dichloropropane, ethyl acetate, which are typical solvents for industrial applications (Li et al., 2020; Huang et al., 2014). Therefore, Factor 6 was assigned to solvent usage 1. The CPF plots of this factor indicated that the northeast and southeast were the dominant directions (Fig. S4f).

The Factor 7 was dominated by methylcyclopentane, cyclohexane, TEXs（Toluene, Ethylbenzene, m/p-Xylene, and o-Xylene）, 1,2-Dichloroethane、1,2-Dichloropropane, and Ethyl acetate. Methylcyclopentane and cyclohexane were commonly used as solvents in industrial processes (Lyu et al., 2016; Yuan et al., 2013). TEX is the main component of organic solvents (Guo et al., 2011; Watson et al., 2001). Therefore, Factor 7 was assigned to solvent usage 2. The CPF plots of this factor indicate that the high CPF values were found near the center when the wind speed was low (≤1 m/s).This finding indicates that local emissions was the dominant source (Fig. S4g).

https://doi.org/10.5194/egusphere-2023-2835
Preprint. Discussion started: 8 January 2024

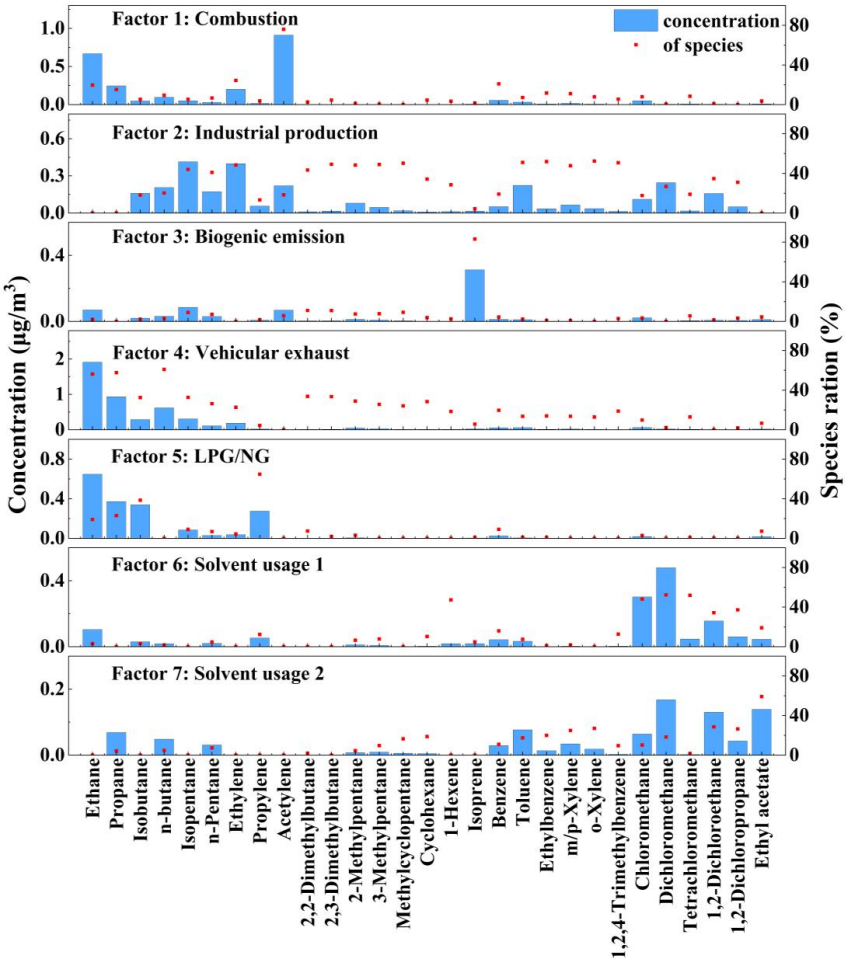

Fig. 4. Source profiles and contributions of VOCs during the observation period.

Figure 5 shows the proportion of each VOCs source during the observation process. In the entire observation period, vehicular exhaust is the main contributor, accounting for 28%, followed by solvent usage (27%) and industrial production (22%). Other sources including LPG/NG (9%), combustion sources (8%), and biogenic emission (6%) contributed little. In Case 1, vehicular exhaust (30%) was the largest contributor, followed by solvent usage (27%) and industrial production (23%). Compared with the Case 1 event, the contribution of solvent usage and industrial production in the Case 2 event did not change much, and the contribution of LPG/NG increased by 14%, which became an important source. On clean days, vehicular exhaust (35%), solvent usage (25%), and industrial production (21%) were the most significant contributors. Compared with clean days, the contribution of solvent usage, industrial production, biogenic emission, and LPN/NG in both pollution events increased, while the contribution of combustion sources and vehicular exhaust decreased. In summary, vehicular exhaust, solvent usage, and industrial production were major contributors to both O_3 pollution events and clean days.

https://doi.org/10.5194/egusphere-2023-2835
Preprint. Discussion started: 8 January 2024

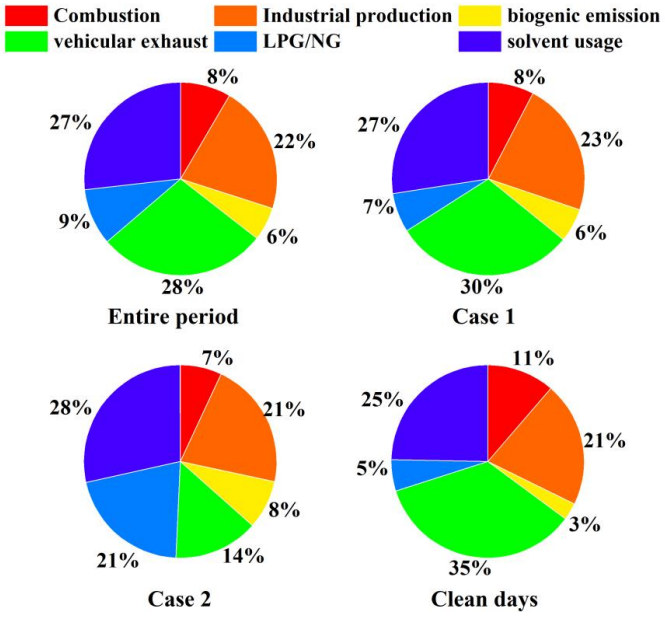

Fig. 5. Source contributions to VOCs concentration during different periods.

3.3 Contribution to O_3 formation

3.3.1 O_3 sensitivity analysis

In this study, the RIR of AVOCs, biogenic VOCs (BVOCs), CO, NO_x, alkanes, alkenes, and aromatics were calculated (Fig. 6). The RIR values of VOCs were all positive during the entire period, indicating that O_3 generation is most sensitive to VOCs reduction. In comparison, the RIR value of NO_x was negative, indicating that reduction of NO_x would cause the increasing of the O_3 concentrations. Among AVOCs, aromatics had the highest RIR value, followed by alkanes and aromatics. For both O_3 pollution events and clean days, the RIR value of NO_x was negative, and the RIR of VOCs and CO were positive. The absolute value of RIR of each group and species in the pollution events was smaller than that in the non-pollution events, indicating that the sensitivity of O_3 to VOCs, NO_x, and CO on clean days was higher than that in the O_3 pollution events. During the entire period, especially in the pollution events, the RIR of AVOCs was lower than that of BVOCs, indicating that biogenic emission was more sensitive to O_3 formation.

https://doi.org/10.5194/egusphere-2023-2835
Preprint. Discussion started: 8 January 2024

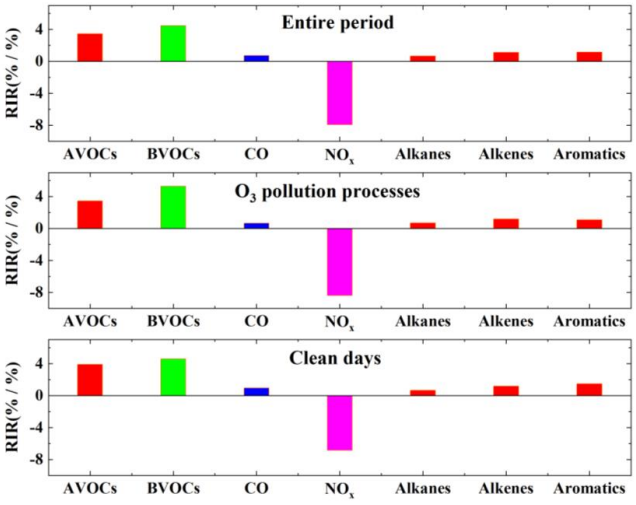

Fig. 6. Average RIR values of the O_3 for different species/groups during different processes in Zhengzhou.

3.3.2 Empirical kinetics modeling approach (EKMA) results

Given the current inability to implement appropriate control measures for BVOCs, the following analysis considers only the impact of AVOCs and NO_x on O_3 formation. The EKMA curve drawn based on the OBM model is shown in Fig. 7. It can be seen from the EKMA curve that O_3 generation presents a highly nonlinear relationship with its precursor compounds AVOCs and NO_x, and the same O_3 concentration can be generated by different concentration combinations of AVOCs and NO_x. In the figure, AVOCs and NO_x = 100% is the base case, and the horizontal and vertical axes represented the percentages of VOCs and NO_x relative to the actual observed mixture ratio (100%). The straight lines in the figure are called ridgeline and is formed by the junction of turning points of O_3 concentration lines (Dodge, 1977).

The ridge divides the graph into the upper left and the lower right parts, and there are also large differences in O_3 generation between these two parts. In the lower right part, each O_3 concentration line and the horizontal coordinate show a parallel relationship. If the NO_x concentration is maintained unchanged, the O_3 concentration does not change with the change of AVOCs concentration. When the AVOCs concentration is unchanged, the concentration of O_3 decreases with the decrease of NO_x concentration. Therefore, in this part of the region, O_3 generation is controlled by NO_x. In the upper left part, if the concentration of AVOCs is reduced alone, the concentration of O_3 will decrease significantly; if only the concentration of NO_x is reduced, the concentration of O_3 will first rise and then decrease. In this region, O_3 generation is in the control region of AVOCs. In the area near the ridge line, when NO_x and AVOCs are reduced at the same time, the O_3 concentration will decrease, and the O_3 generation in the cooperative control area of AVOCs and NO_x.

The ridgeline slope of this EKMA curve was about 6:1, that was, the reduction of NO_x and AVOCs along

https://doi.org/10.5194/egusphere-2023-2835
Preprint. Discussion started: 8 January 2024

this ridge was the fastest way to reduce the O_3 concentration. As can be seen from the figure, Zhengzhou was a typical AVOCs control area, and O_3 was very sensitive to the changes of AVOCs. Therefore, reducing AVOCs can effectively reduce the generation of O_3.

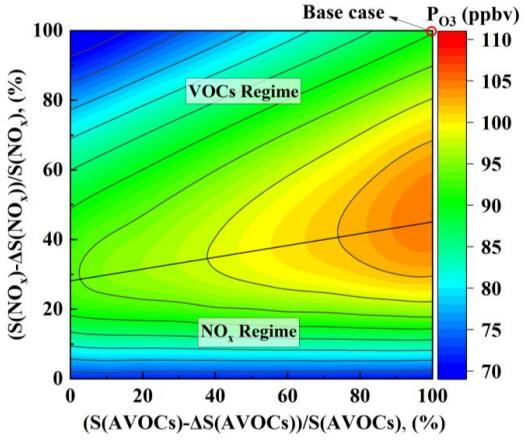

Fig. 7. Isopleth diagram of modeled $P(O_3)$ on S(VOCs) and $S(NO_x)$ remaining percentages.

3.3.3 Control strategies of O_3

The above analysis based on single species (NO_x or AVOCs) is only used to discuss the sensitivity of O_3 concentration to precursor, but such extreme control is difficult to achieve. Usually in the actual operation, the method of simultaneously controlling NO_x and AVOCs emissions is usually adopted to reduce the concentration of O_3. To establish a reasonable and effective VOCs and NO_x emission reduction plan, we further conducted a series of simulations to calculate the net O_3 production rate ($P(O_3)$) by adjusting the ratio of input VOCs and NO_x. The following analyzes the reduction cases of O_3 control at 10 a.m. to 4 p.m. during the observation period.

Figure. 8 shows different reduction schemes. In Fig. 8, the horizontal and vertical axes corresponded to the reduction percentages of NO_x or NO_x + VOCs and the incremental in $P(O_3)$ (positive and negative values represent the increase and decrease of $P(O_3)$ compared to the base case). The results show that $P(O_3)$ will eventually decline regardless of the reduction method, but the trend of change varies (Fig. 8a). As can be seen from Fig. 8b, if only NO_x was reduced, when the emission reduction was less than 60%, the change in $P(O_3)$ shows an increasing trend; when the emission reduction was greater than 60%, the change of $P(O_3)$ shows a decreasing trend. Therefore, only NO_x emission reduction was not conducive to the reduction of $P(O_3)$. When the reduction ratio of AVOCs/NO_x was 1:2 and 1:1, the change in $P(O_3)$ shows a similar trend as that of NO_x emission reduction only, and $P(O_3)$ increases first and then decreases. When the reduction ratio of AVOCs/NO_x was 2:1, $P(O_3)$ increases to a certain extent. When the emission reduction ratio of AVOCs/NO_x was 3:1 or 4:1,

https://doi.org/10.5194/egusphere-2023-2835
Preprint. Discussion started: 8 January 2024

429 $P(O_3)$ continues to decline, and the decline rate of $P(O_3)$ of 4:1 was greater than 3:1. If only AVOCs emission
430 was reduced, $P(O_3)$ shows a continuous downward trend, and the decline rate was very fast. However,
431 combined with actual production activities, only reducing AVOCs emissions cannot be achieved, which was
432 not conducive to policy implementation. Therefore, from the perspective of comprehensive emission reduction
433 effect, the reduction ratio of AVOCs/NO_x should be no less than 3:1, which will be conducive to the reduction
434 of $P(O_3)$.

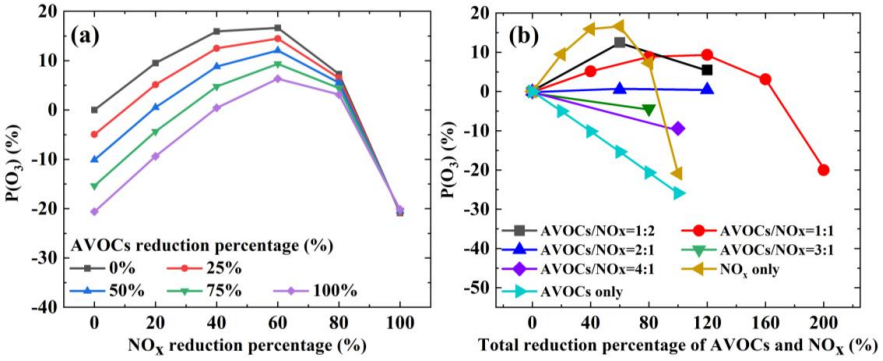

435

436 **Fig. 8.** Response of the $P(O_3)$ to different AVOCs and NO_x reduction percentages. Note: AVOCs/NO_x was the
437 ratio of the percentage reduction of AVOCs and NO_x.

438 In addition, this study analyzed O_3 reduction schemes from 10 a.m. to 4 p.m. It can be seen from Fig. S5
439 that with the reduce of NO_x, $P(O_3)$ elevated and then decreased. When the reduction ratio of AVOCs was fixed
440 and the reduction ratio of NO_x was less than 60%, $P(O_3)$ increases with the reduce of NO_x. In this case, $P(O_3)$
441 increases by 30, 21, 16, 13, 13, 15, and 15% respectively (that is, under the AVOCs scenario without reduction).
442 When the NO_x reduction ratio was greater than 60%, $P(O_3)$ decreases with the reduce of NO_x. When the
443 reduction was the greatest (that is, 100% reduction of NO_x and AVOCs), $P(O_3)$ at 10 o 'clock was still increased
444 compared with the atmospheric observation concentration, increased by 14%; $P(O_3)$ at 11 a.m. to 4 p.m.
445 decreased by 2, 15, 25, 32, 36, and 36%, respectively.

446 Between the range of 10 a.m. to 4 p.m. in the day, when only NO_x was reduced, $P(O_3)$ elevated and then
447 decreased. When only AVOCs were reduced, $P(O_3)$ continued to decrease. When the reduction ratio of
448 AVOCs/NO_x was less than 2:1, $P(O_3)$ elevated and then decreased. When the reduction ratio of AVOCs/NO_x
449 was greater than 2:1, $P(O_3)$ continues to decrease. When AVOCs/NO_x = 4:1, $P(O_3)$ decreases the most and the
450 fastest. According to the reduction ratio of AVOCs/NO_x = 4:1, the maximum reduction of $P(O_3)$ at 10 a.m. to
451 16 p.m. during the day were 3, 6, 10, 11, 13, and 13%, respectively.

452 **4 Conclusions**

453 This study investigated the characteristics and emission sources of VOCs in Zhengzhou from 1st to 30th

https://doi.org/10.5194/egusphere-2023-2835
Preprint. Discussion started: 8 January 2024

June 2023. The OBM was used to analyze the influence of precursors on the formation of O_3, and the emission reduction strategy of precursors was proposed to control the concentration of O_3. The major findings are discussed below.

During the entire period, the concentration of TVOCs varied from 9.9 to 60.3 ppbv, with an average value of 22.9 ± 8.3 ppbv. The average concentration of TVOCs during O_3 pollution was higher than that during clean days. Alkanes (44%), OVOCs (20%), and halocarbons (19%) were the most abundant VOCs group. Ethane, acetone, and propane were always the most abundant species.

Vehicular exhaust (28%), solvent usage (27%), and industrial production (22%) were the main emission sources of VOCs. The contribution of solvent use, industrial production, biogenic emission, and LPN/NG increased during pollution events compared with clean days.

The sensitivity of O_3 formation to its precursor was studied by the OBM method. VOCs had the highest RIR value, while NO_x had a negative RIR value. Olefins have the highest RIR value among AVOCs. It was worth noting that the RIR value of BVOCs was greater than that of AVOCs. The EKMA curve indicated that O_3 formations were in the AVOCs-limited regimes, which means reducing the concentration of AVOCs was an effective way to reduce O_3 concentration. According to the scenario analysis and considering the policy feasibility, the minimum reduction ratio of AVOCs/NO_x should be no less than 3:1 to reduce O_3 production.

Data availability. Data can be obtained upon request from the authors.

Authorship contributions. DZ performed chemical modelling analyses of OBM-MCM and wrote the paper. XL collected the data and contributed to the data analysis. RZ designed and revised the paper. QX, FS, and SW contributed to discussions of results. MY and YX provided part of the data in Zhengzhou.

Competing interests. The contact author has declared that neither they nor their co-authors have any competing interests.

Financial support. This work was supported by National Key Research and Development Program of China (No. 2017YFC0212403).

References

An, J., Zhu, B., Wang, H., Li, Y., Lin, X., and Yang, H.: Characteristics and source apportionment of VOCs measured in an industrial area of Nanjing, Yangtze River Delta, China, Atmos. Environ., 97, 206-214,

https://doi.org/10.5194/egusphere-2023-2835
Preprint. Discussion started: 8 January 2024

https://doi.org/10.1016/j.atmosenv.2014.08.021, 2014.

Andreae, M. O., and Merlet, P.: Emission of trace gases and aerosols from biomass burning, Global. Biogeochem. Cy., 15, 955-966, https://doi.org/10.1029/2000GB001382, 2001.

Barletta, B., Meinardi, S., Sherwood Rowland, F., Chan, C.-Y., Wang, X., Zou, S., Yin Chan, L., and Blake, D. R.: Volatile organic compounds in 43 Chinese cities, Atmos. Environ., 39, 5979-5990, https://doi.org/10.1016/j.atmosenv.2005.06.029, 2005.

Billionnet, C., Gay, E., Kirchner, S., Leynaert, B., and Annesi-Maesano, I.: Quantitative assessments of indoor air pollution and respiratory health in a population-based sample of French dwellings, Environ. Res., 111, 425-434, https://doi.org/10.1016/j.envres.2011.02.008, 2011.

Blake, D. R., and Rowland, F. S.: Urban Leakage of Liquefied Petroleum Gas and Its Impact on Mexico City Air Quality, Science, 269, 953-956, https://doi.org/10.1126/science.269.5226.953, 1995.

Bon, D. M., Ulbrich, I. M., de Gouw, J. A., Warneke, C., Kuster, W. C., Alexander, M. L., Baker, A., Beyersdorf, A. J., Blake, D., Fall, R., Jimenez, J. L., Herndon, S. C., Huey, L. G., Knighton, W. B., Ortega, J., Springston, S., and Vargas, O.: Measurements of volatile organic compounds at a suburban ground site (T1) in Mexico City during the MILAGRO 2006 campaign: measurement comparison, emission ratios, and source attribution, Atmos. Chem. Phys., 11, 2399-2421, https://doi.org/10.5194/acp-11-2399-2011, 2011.

Brown, S. G., Frankel, A., and Hafner, H. R.: Source apportionment of VOCs in the Los Angeles area using Positive Matrix Factorization, Atmos. Environ., 41, 227-237, https://doi.org/10.1016/j.atmosenv.2006.08.021, 2007.

Callén, M. S., Iturmendi, A., and López, J. M.: Source apportionment of atmospheric $PM_{2.5}$-bound polycyclic aromatic hydrocarbons by a PMF receptor model. Assessment of potential risk for human health, Environ. Pollut., 195, 167-177, https://doi.org/10.1016/j.envpol.2014.08.025, 2014.

Cardelino, C. A., and Chameides, W. L.: An observation-based model for analyzing ozone precursor relationships in the urban atmosphere, J. Air. Waste. Manage., 45, 161-180, https://doi.org/10.1080/10473289.1995.10467356, 1995.

Cardelino, C. A., and Chameides, W. L.: The application of data from photochemical assessment monitoring stations to the observation-based model, Atmos. Environ., 34, 2325-2332, https://doi.org/10.1016/S1352-2310(99)00469-0, 2000.

Chameides, W. L., Fehsenfeld, F., Rodgers, M. O., Cardelino, C., Martinez, J., Parrish, D., Lonneman, W., Lawson, D. R., Rasmussen, R. A., Zimmerman, P., Greenberg, J., Middleton, P., and Wang, T.: Ozone

https://doi.org/10.5194/egusphere-2023-2835
Preprint. Discussion started: 8 January 2024

precursor relationships in the ambient atmosphere, J. Geophys. Res-Atmos., 97, 6037-6055, https://doi.org/10.1029/91jd03014, 1992.

Chen, D., Xu, Y., Xu, J., Lian, M., Zhang, W., Wu, W., Wu, M., and Zhao, J.: The Vertical Distribution of VOCs and Their Impact on the Environment: A Review, Atmosphere, 13, 1940, https://doi.org/10.3390/atmos13121940, 2022a.

Chen, D., Zhou, L., Wang, C., Liu, H., Qiu, Y., Shi, G., Song, D., Tan, Q., and Yang, F.: Characteristics of ambient volatile organic compounds during spring O_3 pollution episode in Chengdu, China, J. Environ. Sci., 114, 115-125, https://doi.org/10.1016/j.jes.2021.08.014, 2022b.

Chen, L., Zhu, J., Liao, H., Yang, Y., and Yue, X.: Meteorological influences on $PM_{2.5}$ and O_3 trends and associated health burden since China's clean air actions, Sci. Total. Environ., 744, 140837, https://doi.org/10.1016/j.scitotenv.2020.140837, 2020.

Chen, W. T., Shao, M., Lu, S. H., Wang, M., Zeng, L. M., Yuan, B., and Liu, Y.: Understanding primary and secondary sources of ambient carbonyl compounds in Beijing using the PMF model, Atmos. Chem. Phys., 14, 3047-3062, https://doi.org/10.5194/acp-14-3047-2014, 2014.

Chu, W., Li, H., Ji, Y., Zhang, X., Xue, L., Gao, J., and An, C.: Research on ozone formation sensitivity based on observational methods: Development history, methodology, and application and prospects in China, J. Environ. Sci., 138, 543-560, https://doi.org/10.1016/j.jes.2023.02.052, 2023.

Dai, P., Ge, Y., Lin, Y., Su, S., and Liang, B.: Investigation on characteristics of exhaust and evaporative emissions from passenger cars fueled with gasoline/methanol blends, Fuel, 113, 10-16, https://doi.org/10.1016/j.fuel.2013.05.038, 2013.

Dodge, M. C.: Combined use of modeling techniques and smog chamber data to derive ozone-precursor relationships, Proceedings of the International Conference on Photochemical Oxidant Pollution and Its Control, 2, 881-889, 1977.

Goldberg, D. L., Vinciguerra, T. P., Anderson, D. C., Hembeck, L., Canty, T. P., Ehrman, S. H., Martins, D. K., Stauffer, R. M., Thompson, A. M., Salawitch, R. J., and Dickerson, R. R.: CAMx ozone source attribution in the eastern United States using guidance from observations during DISCOVER - AQ Maryland, Geophys. Res. Lett., 43, 2249-2258, https://doi.org/10.1002/2015gl067332, 2016.

Goldstein, A. H., and Galbally, I. E.: Known and unexplored organic constituents in the earth's atmosphere, Environ. Sci. Technol., 41, 1514-1521, https://doi.org/10.1021/es072476p, 2007.

Guenther, A. B., Zimmerman, P. R., Harley, P. C., Monson, R. K., and Fall, R.: Isoprene and monoterpene emission rate variability: Model evaluations and sensitivity analyses, J. Geophys. Res-Atmos., 98, 12609-

https://doi.org/10.5194/egusphere-2023-2835
Preprint. Discussion started: 8 January 2024

12617, https://doi.org/https://doi.org/10.1029/93JD00527, 1993.

Guo, H., Cheng, H. R., Ling, Z. H., Louie, P. K., and Ayoko, G. A.: Which emission sources are responsible for the volatile organic compounds in the atmosphere of Pearl River Delta?, J. Hazard. Mater., 188, 116-124, https://doi.org/10.1016/j.jhazmat.2011.01.081, 2011.

Guo, H., Ling, Z. H., Cheung, K., Wang, D. W., Simpson, I. J., and Blake, D. R.: Acetone in the atmosphere of Hong Kong: Abundance, sources and photochemical precursors, Atmos. Environ., 65, 80-88, https://doi.org/10.1016/j.atmosenv.2012.10.027, 2013.

He, Z., Li, G., Chen, J., Huang, Y., An, T., and Zhang, C.: Pollution characteristics and health risk assessment of volatile organic compounds emitted from different plastic solid waste recycling workshops, Environ. Int., 77, 85-94, https://doi.org/10.1016/j.envint.2015.01.004, 2015.

Hong, Z., Li, M., Wang, H., Xu, L., Hong, Y., Chen, J., Chen, J., Zhang, H., Zhang, Y., Wu, X., Hu, B., and Li, M.: Characteristics of atmospheric volatile organic compounds (VOCs) at a mountainous forest site and two urban sites in the southeast of China, Sci. Total. Environ., 657, 1491-1500, https://doi.org/10.1016/j.scitotenv.2018.12.132, 2019.

Huang, B., Lei, C., Wei, C., and Zeng, G.: Chlorinated volatile organic compounds (Cl-VOCs) in environment — sources, potential human health impacts, and current remediation technologies, Environ. Int., 71, 118-138, https://doi.org/10.1016/j.envint.2014.06.013, 2014.

Huang, C., Shi, Y., Yang, M., Tong, L., Dai, X., Liu, F., Huang, C., Zheng, J., Li, J., and Xiao, H.: Spatiotemporal distribution, source apportionment and health risk assessment of atmospheric volatile organic compounds using passive air samplers in a typical coastal area, China, J. Clean. Prod., 423, 138741, https://doi.org/10.1016/j.jclepro.2023.138741, 2023.

Huang, J., Fung, J. C. H., Lau, A. K. H., and Qin, Y.: Numerical simulation and process analysis of typhoon-related ozone episodes in Hong Kong, J. Geophys. Res-Atmos., 110, https://doi.org/10.1029/2004jd004914, 2005.

Jorquera, H., and Rappenglück, B.: Receptor modeling of ambient VOC at Santiago, Chile, Atmos. Environ., 38, 4243-4263, https://doi.org/10.1016/j.atmosenv.2004.04.030, 2004.

Kleinman, L. I.: Ozone process insights from field experiments – part II: Observation-based analysis for ozone production, Atmos. Environ., 34, 2023-2033, https://doi.org/https://doi.org/10.1016/S1352-2310(99)00457-4, 2000.

Lerner, J. E. C., Sanchez, E. Y., Sambeth, J. E., and Porta, A. A.: Characterization and health risk assessment of VOCs in occupational environments in Buenos Aires, Argentina, Atmos. Environ., 55, 440-447,

https://doi.org/10.5194/egusphere-2023-2835
Preprint. Discussion started: 8 January 2024

https://doi.org/10.1016/j.atmosenv.2012.03.041, 2012.

Li, J., Zhai, C., Yu, J., Liu, R., Li, Y., Zeng, L., and Xie, S.: Spatiotemporal variations of ambient volatile organic compounds and their sources in Chongqing, a mountainous megacity in China, Sci. Total. Environ., 627, 1442-1452, https://doi.org/10.1016/j.scitotenv.2018.02.010, 2018.

Li, Y., Yin, S., Yu, S., Yuan, M., Dong, Z., Zhang, D., Yang, L., and Zhang, R.: Characteristics, source apportionment and health risks of ambient VOCs during high ozone period at an urban site in central plain, China, Chemosphere, 250, 126283, https://doi.org/10.1016/j.chemosphere.2020.126283, 2020.

Lin, C., Ho, T. C., Chu, H., Yang, H., Chandru, S., Krishnarajanagar, N., Chiou, P., and Hopper, J. R.: Sensitivity analysis of ground-level ozone concentration to emission changes in two urban regions of southeast Texas, J. Environ. Manage., 75, 315-323, https://doi.org/10.1016/j.jenvman.2004.09.012, 2005.

Ling, Z. H., Guo, H., Cheng, H. R., and Yu, Y. F.: Sources of ambient volatile organic compounds and their contributions to photochemical ozone formation at a site in the Pearl River Delta, southern China, Environ. Pollut., 159, 2310-2319, https://doi.org/10.1016/j.envpol.2011.05.001, 2011.

Ling, Z. H., Guo, H., Zheng, J. Y., Louie, P. K. K., Cheng, H. R., Jiang, F., Cheung, K., Wong, L. C., and Feng, X. Q.: Establishing a conceptual model for photochemical ozone pollution in subtropical Hong Kong, Atmos. Environ., 76, 208-220, https://doi.org/10.1016/j.atmosenv.2012.09.051, 2013.

Liu, B., Liang, D., Yang, J., Dai, Q., Bi, X., Feng, Y., Yuan, J., Xiao, Z., Zhang, Y., and Xu, H.: Characterization and source apportionment of volatile organic compounds based on 1-year of observational data in Tianjin, China, Environ. Pollut., 218, 757-769, https://doi.org/10.1016/j.envpol.2016.07.072, 2016.

Liu, B., Yang, Y., Yang, T., Dai, Q., Zhang, Y., Feng, Y., and Hopke, P. K.: Effect of photochemical losses of ambient volatile organic compounds on their source apportionment, Environ. Int., 172, 107766, https://doi.org/10.1016/j.envint.2023.107766, 2023a.

Liu, T., Hong, Y., Li, M., Xu, L., Chen, J., Bian, Y., Yang, C., Dan, Y., Zhang, Y., Xue, L., Zhao, M., Huang, Z., and Wang, H.: Atmospheric oxidation capacity and ozone pollution mechanism in a coastal city of southeastern China: analysis of a typical photochemical episode by an observation-based model, Atmos. Chem. Phys., 22, 2173-2190, https://doi.org/10.5194/acp-22-2173-2022, 2022.

Liu, Y., Shao, M., Fu, L., Lu, S., Zeng, L., and Tang, D.: Source profiles of volatile organic compounds (VOCs) measured in China: Part I, Atmos. Environ., 42, 6247-6260, https://doi.org/10.1016/j.atmosenv.2008.01.070, 2008.

Liu, Y., Song, M., Liu, X., Zhang, Y., Hui, L., Kong, L., Zhang, Y., Zhang, C., Qu, Y., An, J., Ma, D., Tan, Q., and Feng, M.: Characterization and sources of volatile organic compounds (VOCs) and their related

https://doi.org/10.5194/egusphere-2023-2835
Preprint. Discussion started: 8 January 2024

changes during ozone pollution days in 2016 in Beijing, China, Environ. Pollut., 257, 113599, https://doi.org/10.1016/j.envpol.2019.113599, 2020.

Liu, Y., Kong, L., Liu, X., Zhang, Y., Li, C., Zhang, Y., Zhang, C., Qu, Y., An, J., Ma, D., Tan, Q., Feng, M., and Zha, S.: Characteristics, secondary transformation, and health risk assessment of ambient volatile organic compounds (VOCs) in urban Beijing, China, Atmos. Pollut. Res., 12, 33-46, https://doi.org/10.1016/j.apr.2021.01.013, 2021.

Liu, Z., Hu, K., Zhang, K., Zhu, S., Wang, M., and Li, L.: VOCs sources and roles in O_3 formation in the central Yangtze River Delta region of China, Atmos. Environ., 302, 119755, https://doi.org/10.1016/j.atmosenv.2023.119755, 2023b.

Liu, Z., Wang, B., Wang, C., Sun, Y., Zhu, C., Sun, L., Yang, N., Fan, G., Sun, X., Xia, Z., Pan, G., Zhu, C., Gai, Y., Wang, X., Xiao, Y., Yan, G., and Xu, C.: Characterization of photochemical losses of volatile organic compounds and their implications for ozone formation potential and source apportionment during summer in suburban Jinan, China, Environ. Res., 238, 117158, https://doi.org/10.1016/j.envres.2023.117158, 2023c.

Lu, B., Zhang, Z., Jiang, J., Meng, X., Liu, C., Herrmann, H., Chen, J., Xue, L., and Li, X.: Unraveling the O_3-NO_x-VOCs relationships induced by anomalous ozone in industrial regions during COVID-19 in Shanghai, Atmos. Environ., 308, 119864, https://doi.org/10.1016/j.atmosenv.2023.119864, 2023.

Lyu, X. P., Chen, N., Guo, H., Zhang, W. H., Wang, N., Wang, Y., and Liu, M.: Ambient volatile organic compounds and their effect on ozone production in Wuhan, central China, Sci. Total. Environ., 541, 200-209, https://doi.org/10.1016/j.scitotenv.2015.09.093, 2016.

Miller, L., Xu, X., Grgicak-Mannion, A., Brook, J., and Wheeler, A.: Multi-season, multi-year concentrations and correlations amongst the BTEX group of VOCs in an urbanized industrial city, Atmos. Environ., 61, 305-315, https://doi.org/10.1016/j.atmosenv.2012.07.041, 2012.

Min, R., Wang, F., Wang, Y., Song, G., Zheng, H., Zhang, H., Ru, X., and Song, H.: Contribution of local and surrounding area anthropogenic emissions to a high ozone episode in Zhengzhou, China, Environ. Res., 212, 113440, https://doi.org/10.1016/j.envres.2022.113440, 2022.

Mo, Z., Shao, M., Lu, S., Qu, H., Zhou, M., Sun, J., and Gou, B.: Process-specific emission characteristics of volatile organic compounds (VOCs) from petrochemical facilities in the Yangtze River Delta, China, Sci. Total. Environ., 533, 422-431, https://doi.org/10.1016/j.scitotenv.2015.06.089, 2015.

Monod, A., Sive, B. C., Avino, P., Chen, T., Blake, D. R., and Sherwood Rowland, F.: Monoaromatic compounds in ambient air of various cities: a focus on correlations between the xylenes and ethylbenzene,

https://doi.org/10.5194/egusphere-2023-2835
Preprint. Discussion started: 8 January 2024

Atmos. Environ., 35, 135-149, https://doi.org/https://doi.org/10.1016/S1352-2310(00)00274-0, 2001.

Mozaffar, A., Zhang, Y., Fan, M., Cao, F., and Lin, Y.: Characteristics of summertime ambient VOCs and their contributions to O_3 and SOA formation in a suburban area of Nanjing, China, Atmos. Res., 240, 104923, https://doi.org/10.1016/j.atmosres.2020.104923, 2020.

Mozaffar, A., Zhang, Y., Lin, Y., Xie, F., Fan, M., and Cao, F.: Measurement report: High contributions of halocarbon and aromatic compounds to atmospheric volatile organic compounds in an industrial area, Atmos. Chem. Phys., 21, 18087-18099, https://doi.org/10.5194/acp-21-18087-2021, 2021.

The number of motor vehicles in China exceeded 400 million: https://www.mps.gov.cn/n2254314/n6409334/c8451247/content.html, 2022.

Na, K., Kim, Y. P., Moon, K.-C., Moon, I., and Fung, K.: Concentrations of volatile organic compounds in an industrial area of Korea, Atmos. Environ., 35, 2747-2756, https://doi.org/https://doi.org/10.1016/S1352-2310(00)00313-7, 2001.

Nelson, B. S., Stewart, G. J., Drysdale, W. S., Newland, M. J., Vaughan, A. R., Dunmore, R. E., Edwards, P. M., Lewis, A. C., Hamilton, J. F., and Acton, W. J.: In situ ozone production is highly sensitive to volatile organic compounds in Delhi, India, Copernicus Publications, 17, https://doi.org/10.5194/ACP-21-13609-2021, 2021.

Nopmongcol, U., Koo, B., Tai, E., Jung, J., Piyachaturawat, P., Emery, C., Yarwood, G., Pirovano, G., Mitsakou, C., and Kallos, G.: Modeling Europe with CAMx for the Air Quality Model Evaluation International Initiative (AQMEII), Atmos. Environ., 53, 177-185, https://doi.org/https://doi.org/10.1016/j.atmosenv.2011.11.023, 2012.

Norris, G., Duvall, R., Brown, S., and Bai, S.: EPA Positive Matrix Factorization (PMF) 5.0. Fundamentals and User Guide Prepared for the U.S. Environmental Protection Agency Office of Research and Development, Washington, DC (EPA/600/R-14/108; STI-9105115594-UG, April), 2014.

Pacifico, F., Harrison, S. P., Jones, C. D., and Sitch, S.: Isoprene emissions and climate, Atmos. Environ., 43, 6121-6135, https://doi.org/10.1016/j.atmosenv.2009.09.002, 2009.

Prendez, M., Carvajal, V., Corada, K., Morales, J., Alarcon, F., and Peralta, H.: Biogenic volatile organic compounds from the urban forest of the Metropolitan Region, Chile, Environ. Pollut., 183, 143-150, https://doi.org/10.1016/j.envpol.2013.04.003, 2013.

Qiao, X., Sun, M., Wang, Y., Zhang, D., Zhang, R., Zhao, B., and Zhang, J.: Strong relations of peroxyacetyl nitrate (PAN) formation to alkene and nitrous acid during various episodes, Environ. Pollut., 326, 121465, https://doi.org/10.1016/j.envpol.2023.121465, 2023.

https://doi.org/10.5194/egusphere-2023-2835
Preprint. Discussion started: 8 January 2024

671 Ring, A. M., Canty, T. P., Anderson, D. C., Vinciguerra, T. P., He, H., Goldberg, D. L., Ehrman, S. H.,
672 Dickerson, R. R., and Salawitch, R. J.: Evaluating commercial marine emissions and their role in air
673 quality policy using observations and the CMAQ model, Atmos. Environ., 173, 96-107,
674 https://doi.org/10.1016/j.atmosenv.2017.10.037, 2018.
675 Seila, R. L., Main, H. H., Arriaga, J. L., Martínez V, G., and Ramadan, A. B.: Atmospheric volatile organic
676 compound measurements during the 1996 Paso del Norte Ozone Study, Sci. Total. Environ., 276, 153-
677 169, https://doi.org/https://doi.org/10.1016/S0048-9697(01)00777-X, 2001.
678 Sha, Q., Zhu, M., Huang, H., Wang, Y., Huang, Z., Zhang, X., Tang, M., Lu, M., Chen, C., Shi, B., Chen, Z.,
679 Wu, L., Zhong, Z., Li, C., Xu, Y., Yu, F., Jia, G., Liao, S., Cui, X., Liu, J., and Zheng, J.: A newly integrated
680 dataset of volatile organic compounds (VOCs) source profiles and implications for the future development
681 of VOCs profiles in China, Sci. Total. Environ., 793, 148348,
682 https://doi.org/10.1016/j.scitotenv.2021.148348, 2021.
683 Shao, M., Zhang, Y., Zeng, L., Tang, X., Zhang, J., Zhong, L., and Wang, B.: Ground-level ozone in the Pearl
684 River Delta and the roles of VOC and NO(x) in its production, J. Environ. Manage., 90, 512-518,
685 https://doi.org/10.1016/j.jenvman.2007.12.008, 2009.
686 Shao, P., An, J., Xin, J., Wu, F., Wang, J., Ji, D., and Wang, Y.: Source apportionment of VOCs and the
687 contribution to photochemical ozone formation during summer in the typical industrial area in the Yangtze
688 River Delta, China, Atmos. Res., 176-177, 64-74, https://doi.org/10.1016/j.atmosres.2016.02.015, 2016.
689 Sicard, P., De Marco, A., Agathokleous, E., Feng, Z., Xu, X., Paoletti, E., Rodriguez, J. J. D., and Calatayud,
690 V.: Amplified ozone pollution in cities during the COVID-19 lockdown, Sci. Total. Environ., 735, 139542,
691 https://doi.org/10.1016/j.scitotenv.2020.139542, 2020.
692 Song, Y., Shao, M., Liu, Y., Lu, S., Kuster, W., Goldan, P., and Xie, S.: Source apportionment of ambient
693 volatile organic compounds in Beijing, Environ. Sci. Technol. , 41, 4348-4353, 2007.
694 Tang, J. H., Chan, L. Y., Chan, C. Y., Li, Y. S., Chang, C. C., Liu, S. C., Wu, D., and Li, Y. D.: Characteristics
695 and diurnal variations of NMHCs at urban, suburban, and rural sites in the Pearl River Delta and a remote
696 site in South China, Atmos. Environ., 41, 8620-8632, https://doi.org/10.1016/j.atmosenv.2007.07.029,
697 2007.
698 Thijsse, T. R., Oss, R. F. V., and Lenschow, P.: Determination of Source Contributions to Ambient Volatile
699 Organic Compound Concentrations in Berlin, J. Air. Waste. Manage., 49, 1394-1404,
700 https://doi.org/10.1080/10473289.1999.10463974, 1999.
701 Tsai, W. Y., Chan, L. Y., Blake, D. R., and Chu, K. W.: Vehicular fuel composition and atmospheric emissions

https://doi.org/10.5194/egusphere-2023-2835
Preprint. Discussion started: 8 January 2024

in South China: Hong Kong, Macau, Guangzhou, and Zhuhai, Atmos. Chem. Phys., 6, 3281-3288, https://doi.org/10.5194/acp-6-3281-2006, 2006.

Positive Matrix Factorization Model for environmental data analyses: https://www.epa.gov/airr-esearch/positive-matrix-factorization-modelenvironmentaldata-analyses, access: June, 2014.

Wang, B., Liu, Z., Li, Z., Sun, Y., Wang, C., Zhu, C., Sun, L., Yang, N., Bai, G., Fan, G., Sun, X., Xia, Z., Pan, G., Xu, C., and Yan, G.: Characteristics, chemical transformation and source apportionment of volatile organic compounds (VOCs) during wintertime at a suburban site in a provincial capital city, east China, Atmos. Environ., 298, 119621, https://doi.org/10.1016/j.atmosenv.2023.119621, 2023a.

Wang, M., Sheng, H., Liu, Y., Wang, G., Huang, H., Fan, L., and Ye, D.: Research on the diurnal variation characteristics of ozone formation sensitivity and the impact of ozone pollution control measures in "2 + 26" cities of Henan Province in summer, Sci. Total. Environ., 888, 164121, https://doi.org/10.1016/j.scitotenv.2023.164121, 2023b.

Wang, X., Yin, S., Zhang, R., Yuan, M., and Ying, Q.: Assessment of summertime O_3 formation and the O_3-NO_x-VOC sensitivity in Zhengzhou, China using an observation-based model, Sci. Total. Environ., 813, 152449, https://doi.org/10.1016/j.scitotenv.2021.152449, 2022.

Watson, J. G., Chow, J. C., and Fujita, E. M.: Review of volatile organic compound source apportionment by chemical mass balance, Atmos. Environ., 35, 1567-1584, https://doi.org/10.1016/S1352-2310(00)00461-1, 2001.

Wu, R., Li, J., Hao, Y., Li, Y., Zeng, L., and Xie, S.: Evolution process and sources of ambient volatile organic compounds during a severe haze event in Beijing, China, Sci. Total. Environ., 560-561, 62-72, https://doi.org/10.1016/j.scitotenv.2016.04.030, 2016.

Wu, Y., Fan, X., Liu, Y., Zhang, J., Wang, H., Sun, L., Fang, T., Mao, H., Hu, J., Wu, L., Peng, J., and Wang, S.: Source apportionment of VOCs based on photochemical loss in summer at a suburban site in Beijing, Atmos. Environ., 293, https://doi.org/10.1016/j.atmosenv.2022.119459, 2023.

Xia, L., Cai, C., Zhu, B., An, J., Li, Y., and Li, Y.: Source apportionment of VOCs in a suburb of Nanjing, China, in autumn and winter, J. Atmos. Chem., 71, 175-193, https://doi.org/10.1007/s10874-014-9289-6, 2014.

Xie, Y., and Berkowitz, C. M.: The use of positive matrix factorization with conditional probability functions in air quality studies: An application to hydrocarbon emissions in Houston, Texas, Atmos. Environ., 40, 3070-3091, https://doi.org/10.1016/j.atmosenv.2005.12.065, 2006.

Xie, Y., Cheng, C., Wang, Z., Wang, K., Wang, Y., Zhang, X., Li, X., Ren, L., Liu, M., and Li, M.: Exploration

https://doi.org/10.5194/egusphere-2023-2835
Preprint. Discussion started: 8 January 2024

of O_3-precursor relationship and observation-oriented O_3 control strategies in a non-provincial capital city, southwestern China, Sci. Total. Environ., 800, 149422, https://doi.org/10.1016/j.scitotenv.2021.149422, 2021.

Xu, Z., Zou, Q., Jin, L., Shen, Y., Shen, J., Xu, B., Qu, F., Zhang, F., Xu, J., Pei, X., Xie, G., Kuang, B., Huang, X., Tian, X., and Wang, Z.: Characteristics and sources of ambient Volatile Organic Compounds (VOCs) at a regional background site, YRD region, China: Significant influence of solvent evaporation during hot months, Sci. Total. Environ., 857, 159674, https://doi.org/10.1016/j.scitotenv.2022.159674, 2023.

Yan, D., Zhang, Z., Jin, Z., Li, M., Sheridan, S. C., and Wang, T.: Ozone variability driven by the synoptic patterns over China during 2014–2022 and its implications for crop yield and economy, Atmos. Pollut. Res., 14, 101843, https://doi.org/10.1016/j.apr.2023.101843, 2023.

Yang, L., Yuan, Z., Luo, H., Wang, Y., Xu, Y., Duan, Y., and Fu, Q.: Identification of long-term evolution of ozone sensitivity to precursors based on two-dimensional mutual verification, Sci. Total. Environ., 760, 143401, https://doi.org/10.1016/j.scitotenv.2020.143401, 2021.

Yu, S., Su, F., Yin, S., Wang, S., Xu, R., He, B., Fan, X., Yuan, M., and Zhang, R.: Characterization of ambient volatile organic compounds, source apportionment, and the ozone-NO_x-VOC sensitivities in a heavily polluted megacity of central China: effect of sporting events and emission reductions, Atmos. Chem. Phys., 21, 15239-15257, https://doi.org/10.5194/acp-21-15239-2021, 2021.

Yuan, B., Shao, M., de Gouw, J., Parrish, D. D., Lu, S., Wang, M., Zeng, L., Zhang, Q., Song, Y., Zhang, J., and Hu, M.: Volatile organic compounds (VOCs) in urban air: How chemistry affects the interpretation of positive matrix factorization (PMF) analysis, J. Geophys. Res-Atmos., 117, 24302, https://doi.org/10.1029/2012jd018236, 2012.

Yuan, Z., Zhong, L., Lau, A. K. H., Yu, J. Z., and Louie, P. K. K.: Volatile organic compounds in the Pearl River Delta: Identification of source regions and recommendations for emission-oriented monitoring strategies, Atmos. Environ., 76, 162-172, https://doi.org/10.1016/j.atmosenv.2012.11.034, 2013.

Yurdakul, S., Civan, M., Kuntasal, Ö., Doğan, G., Pekey, H., and Tuncel, G.: Temporal variations of VOC concentrations in Bursa atmosphere, Atmos. Pollut. Res., 9, 189-206, https://doi.org/10.1016/j.apr.2017.09.004, 2018.

Zeng, X., Han, M., Ren, G., Liu, G., Wang, X., Du, K., Zhang, X., and Lin, H.: A comprehensive investigation on source apportionment and multi-directional regional transport of volatile organic compounds and ozone in urban Zhengzhou, Chemosphere, 334, 139001, https://doi.org/10.1016/j.chemosphere.2023.139001, 2023.

https://doi.org/10.5194/egusphere-2023-2835
Preprint. Discussion started: 8 January 2024

764 Zhang, D., He, B., Yuan, M., Yu, S., Yin, S., and Zhang, R.: Characteristics, sources and health risks
765 assessment of VOCs in Zhengzhou, China during haze pollution season, J. Environ. Sci., 108, 44-57,
766 https://doi.org/10.1016/j.jes.2021.01.035, 2021.
767 Zhang, H., Wang, Y., Hu, J., Ying, Q., and Hu, X. M.: Relationships between meteorological parameters and
768 criteria air pollutants in three megacities in China, Environ. Res., 140, 242-254,
769 https://doi.org/10.1016/j.envres.2015.04.004, 2015.
770 Zhang, L., Li, H., Wu, Z., Zhang, W., Liu, K., Cheng, X., Zhang, Y., Li, B., and Chen, Y.: Characteristics of
771 atmospheric volatile organic compounds in urban area of Beijing: Variations, photochemical reactivity
772 and source apportionment, J. Environ. Sci., 95, 190-200, https://doi.org/10.1016/j.jes.2020.03.023, 2020.
773 Zhang, Y., Li, R., Fu, H., Zhou, D., and Chen, J.: Observation and analysis of atmospheric volatile organic
774 compounds in a typical petrochemical area in Yangtze River Delta, China, J. Environ. Sci., 71, 233-248,
775 https://doi.org/10.1016/j.jes.2018.05.027, 2018.
776 Zhang, Y. H., Su, H., Zhong, L. J., Cheng, Y. F., Zeng, L. M., Wang, X. S., Xiang, Y. R., Wang, J. L., Gao, D.
777 F., and Shao, M.: Regional ozone pollution and observation-based approach for analyzing ozone–
778 precursor relationship during the PRIDE-PRD2004 campaign, Atmos. Environ., 42, 6203-6218,
779 https://doi.org/10.1016/j.atmosenv.2008.05.002, 2008.
780 Zhang, Z., Zhang, Y., Wang, X., Lü, S., Huang, Z., Huang, X., Yang, W., Wang, Y., and Zhang, Q.:
781 Spatiotemporal patterns and source implications of aromatic hydrocarbons at six rural sites across China's
782 developed coastal regions, J. Geophys. Res-Atmos., 121, 6669-6687,
783 https://doi.org/10.1002/2016jd025115, 2016.
784 Zhang, Z., Sun, Y., and Li, J.: Characteristics and sources of VOCs in a coastal city in eastern China and the
785 implications in secondary organic aerosol and O_3 formation, Sci. Total. Environ., 887, 164117,
786 https://doi.org/10.1016/j.scitotenv.2023.164117, 2023.
787 Zhao, C., Sun, Y., Zhong, Y., Xu, S., Liang, Y., Liu, S., He, X., Zhu, J., Shibamoto, T., and He, M.: Spatio-
788 temporal analysis of urban air pollutants throughout China during 2014-2019, Air. Qual. Atmos. Hlth., 14,
789 1619-1632, https://doi.org/10.1007/s11869-021-01043-5, 2021.
790 Zhu, B., Huang, X., Xia, S., Lin, L., Cheng, Y., and He, L.: Biomass-burning emissions could significantly
791 enhance the atmospheric oxidizing capacity in continental air pollution, Environ. Pollut., 285, 117523,
792 https://doi.org/10.1016/j.envpol.2021.117523, 2021.
793 Zou, Y., Yan, X. L., Flores, R. M., Zhang, L. Y., Yang, S. P., Fan, L. Y., Deng, T., Deng, X. J., and Ye, D. Q.:
794 Source apportionment and ozone formation mechanism of VOCs considering photochemical loss in

https://doi.org/10.5194/egusphere-2023-2835
Preprint. Discussion started: 8 January 2024

795 Guangzhou, China, Sci. Total. Environ., 903, 166191, https://doi.org/10.1016/j.scitotenv.2023.166191,
796 2023.
797
798